2010 IEEE International Conference on Robotics and Automation
Anchorage Convention District
May 3-8, 2010, Anchorage, Alaska, USA

Optimization of the prestress stable wrench closure workspace of planar parallel three-degree-of-freedom cable-driven mechanisms with four cables

Marc Arsenault, *Member*, *IEEE*

Abstract— **There exist configurations of parallel cable-driven mechanisms (CDM) within their wrench closure workspace (WCW) for which they may become unstable when their cables are subjected to internal forces due to prestress or external loads. With the goal of avoiding such configurations, the prestress stable WCW (PSWCW) is defined as a subset of the WCW where an increase in the prestress level leads to an increase in the overall stiffness of the mechanism. A genetic algorithm is used to optimize the geometry of planar parallel CDMs with four cables with the objective of reaching a desired PSWCW. Results are obtained that may guide the designer in the preliminary selection of mechanism dimensions and cable connectivities.**

I. INTRODUCTION

A planar parallel cable-driven mechanism (CDM) consists of a rigid end-effector (EE) that is constrained to move in a plane and is linked to a fixed base by cables acting in parallel. Each cable is attached to the EE at one end and wound around an actuated winch at the other. By modifying the lengths of the cables, the pose (*i.e.*, position and orientation) of the EE in the plane can be controlled. Cable-driven mechanisms are attractive due to the low inertia of their moving parts and the relative ease with which they can be built, transported and reconfigured. However, the fact that the cables can only pull and not push on the EE introduces challenges in the design and use of these mechanisms. To maintain rigidity, the cables must be kept taut at all times. Completely restrained parallel manipulators (CRPM) [1], on which this paper is focused, accomplish this by applying antagonistic tension forces in the cables (*i.e.*, forces whose resultant wrench on the EE is zero). This was shown in [1] to be possible only when $m > n$ where m is the number of cables in the mechanism and n is the number of degrees of freedom of the space in which its EE is displaced (*i.e.*, $n = 3$ in the plane and $n = 6$ in space). The results given in this paper are limited to the case where $m = 4$ cables are used.

Because large lengths of cable can be stored on winches, CDMs have potentially large ranges of motion. However, the portion of this range that is usable, referred to as the mechanism's workspace, is significantly limited by the unilaterality of the forces applied by the cables to the EE. Because of this, it is of primary interest to maximize the size of the workspace of CDMs. Different characterizations exist for the workspace of CDMs [2, 3]. One of these is referred to as the wrench closure workspace (WCW) [4] and is defined as the set of mechanism configurations for which any arbitrary wrench can be generated at the EE with non-negative cable tensions. If the mechanical properties of a CDM's cables, actuators and remaining structure are assumed limitless, the WCW can be shown to depend only on the mechanism's geometry.

In addition to being capable of generating arbitrary wrenches with its EE, the CDM should also be stable. A given pose is considered stable if any arbitrary displacement of the EE away from the pose due to an externally applied disturbance wrench while keeping the cable rest lengths fixed leads to an increase of the total elastic potential energy in the cables. This will be verified if the stiffness matrix of the CDM, evaluated at the stated pose, is positive definite. It is known that the stiffness matrix of CDMs depends both on the axial stiffness of the individual cables as well as on the internal forces in the cables due to the application of prestress and/or to external wrenches applied to the EE [5–7]. Behzadipour and Khajepour [6] have shown, based on a previous work by Svinin *et al.* [8], that whereas the portion of the stiffness matrix corresponding to the axial stiffness of the cables is always positive definite, this is not necessarily true for the internal forces' contribution to the stiffness matrix. In the case of the internal forces due to the prestress in the cables, such behaviour is generally undesirable since prestress is used to keep the cables taut and, ideally, to increase the overall stiffness of the mechanism. With this in mind, this paper examines the effects of the geometry of CDMs on their *prestress stable wrench closure workspace* (PSWCW) which is the subset of the WCW where an increase of the prestress in the cables tends to stabilize the mechanism.

II. KINEMATIC AND STATIC ANALYSIS

A diagram of the CDM to be studied in this paper is shown in Fig. 1. The EE, constrained to move in a plane, is defined by nodes B_i (in this paper $i = 1, 2, 3, 4$) while the base is defined by nodes A_i. Each A_i node is connected to its respective B_i node by a cable whose rest length can be controlled with a motor-driven winch located at node A_i. The ith cable is assumed to be taut such that it can be considered

This work was supported by the Natural Sciences and Engineering Research Council of Canada (NSERC).

The author is with the Department of Mechanical Engineering, Royal Military College of Canada, Kingston, Ontario, Canada, K7K 7B4, marc.arsenault@rmc.ca.

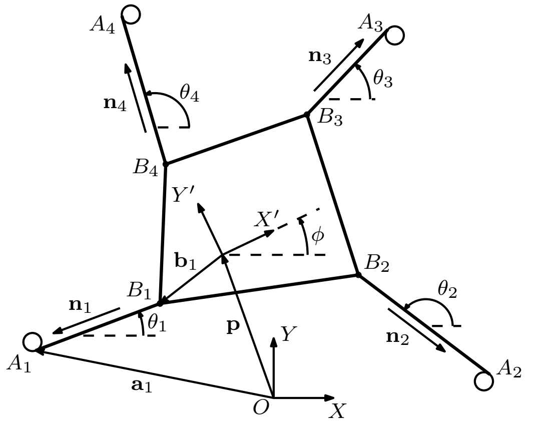

Fig. 1. Planar parallel 3-DoF cable-driven mechanism with four cables.

as a segment of length l_i of the straight line passing through A_i and B_i. The contact points of the cables on the base and EE are considered fixed relative to the respective bodies and are represented as revolute joints with axes perpendicular to the plane of the mechanism.

Reference frames OXY and $PX'Y'$ are defined as being attached to the base and EE, respectively, and are referred to as the base and mobile frames. The position of the EE is given by a vector $\mathbf{p} = [x, y]^T$ directed from point O to point P while its orientation is given by the angle ϕ measured from X to X' about Z. Vector $\mathbf{a}_i$ is defined as being directed from point O to point A_i and is constant in the base frame. Similarly, vector $\mathbf{b}'_i$ is directed from point P to point B_i and is constant in the mobile frame. Unit vector $\mathbf{n}_i$ is defined along the ith cable directed from B_i to A_i and can be expressed as

$$\mathbf{n}_i = \frac{1}{l_i}(\mathbf{a}_i - \mathbf{p} - \mathbf{b}_i). \tag{1}$$

where $\mathbf{b}_i = \mathbf{Q}\mathbf{b}'_i$ and where

$$\mathbf{Q} = \begin{bmatrix} \cos\phi & -\sin\phi \\ \sin\phi & \cos\phi \end{bmatrix} \tag{2}$$

is the rotation matrix bringing frame XY parallel to frame $X'Y'$.

Given t_i the tension in the ith cable, the wrench applied by the latter on the EE is defined as the combination of a force $t_i\mathbf{n}_i$ passing through P and a moment $t_i\mathbf{b}_i^T\mathbf{E}^T\mathbf{n}_i$ about an axis perpendicular to the plane of the mechanism and passing through point P where

$$\mathbf{E} = \begin{bmatrix} 0 & -1 \\ 1 & 0 \end{bmatrix}. \tag{3}$$

It is noted that the expression used to compute the moment applied to the EE by the ith cable is chosen due to its compactness (the moment cannot be expressed as $t_i\mathbf{b}_i \times \mathbf{n}_i$ since $\mathbf{b}_i, \mathbf{n}_i \in \Re^2$). The ith cable's wrench can also be expressed as $t_i\mathbf{w}_i$ where

$$\mathbf{w}_i = \begin{bmatrix} \mathbf{n}_i \\ \mathbf{b}_i^T\mathbf{E}^T\mathbf{n}_i \end{bmatrix} \tag{4}$$

and where it is noted that $t_i \geq 0$ by definition. The total wrench applied to the EE by the cables is then the sum of the individual cable contributions given by $\mathbf{w} = \mathbf{W}\mathbf{t}$ where $\mathbf{W} = [\mathbf{w}_1, \mathbf{w}_2, \mathbf{w}_3, \mathbf{w}_4]$ is defined as the wrench matrix and where $\mathbf{t} = [t_1, t_2, t_3, t_4]^T$. Meanwhile, the total wrench applied to the EE by the environment (including the weight of the EE if applicable) is the combination of a force $\mathbf{f}$ and a moment M, both referenced to point P. The static equilibrium equations of the EE can thus be expressed as

$$\mathbf{f} + \sum_{i=1}^{4} t_i\mathbf{n}_i = \mathbf{0} \tag{5}$$

$$M + \sum_{i=1}^{4} t_i\mathbf{b}_i^T\mathbf{E}^T\mathbf{n}_i = 0 \tag{6}$$

and the total external wrench can also be written as $\mathbf{w}_e = [\mathbf{f}, M]^T$ where $\mathbf{w}_e = -\mathbf{w}$.

III. COMPUTATION OF THE WRENCH CLOSURE WORKSPACE

Generally speaking, the workspace of a CDM is constrained by the cables' mechanical limits as well as the mechanism's ability to generate a specified set of required wrenches at its EE. The WCW, as defined by Gouttefarde and Gosselin [4], assumes both the mechanical limits of the cables and the set of required wrenches as unbounded. As a result of these assumptions, which are deemed reasonable in a preliminary design setting where the optimal geometry of the mechanism is sought, the WCW depends solely on the geometry of the mechanism. In what follows, for any vector $\mathbf{q}$, the expressions $\mathbf{q} > \mathbf{0}$, $\mathbf{q} \geq \mathbf{0}$ and $\mathbf{q} < \mathbf{0}$ are to be interpreted as all components of $\mathbf{q}$ being greater than zero, greater than or equal to zero, or less than zero, respectively.

The WCW of planar CDMs can formally be defined as the set of EE poses for which, given any wrench $\mathbf{w} \in \Re^3$, there exists a vector $\mathbf{t} \geq 0$ such that $\mathbf{w} = \mathbf{W}\mathbf{t}$ is satisfied. Recalling that $m > n$, the static equilibrium equation of a CDM (*i.e.*, $\mathbf{w} = \mathbf{W}\mathbf{t}$) is an underdetermined system whose solution can be expressed as

$$\mathbf{t} = \mathbf{t}_\mathbf{w} + \mathbf{t}_0 = \mathbf{W}^I\mathbf{w} + \lambda\mathbf{z} \tag{7}$$

where $\mathbf{W}^I$ is the generalized inverse of $\mathbf{W}$, $\lambda \in \Re$ and $\mathbf{z}$ is in the nullspace of $\mathbf{W}$. The cable tensions are thus viewed as a combination of $\mathbf{t}_\mathbf{w} = \mathbf{W}^I\mathbf{w}$, corresponding to the tensions required to equilibrate the wrench applied to the EE, and $\mathbf{t}_0 = \lambda\mathbf{z}$, which are the prestress cable forces whose resultant wrench on the EE is zero. With this solution in mind, necessary and sufficient conditions for a given pose to belong to the WCW are (taken from [4])

$$\text{rank}(\mathbf{W}) = 3 \tag{8}$$

$$\exists\ \mathbf{z} \in \text{null}(\mathbf{W}) \text{ such that } \mathbf{z} > \mathbf{0} \tag{9}$$

where rank($\mathbf{W}$) and null($\mathbf{W}$) correspond to the rank and nullspace of $\mathbf{W}$, respectively. When these conditions are satisfied, the cable tensions can be made positive by adjusting the value of λ without having any effect on the wrench generated at the EE. In order to verify (9), a unit vector $\mathbf{z}_0$ in the nullspace of $\mathbf{W}$ is obtained as the fourth column of $\mathbf{V}$ in the singular value decomposition of $\mathbf{W}$ which takes the form $\mathbf{W} = \mathbf{U}\Sigma\mathbf{V}^T$ where $\mathbf{U}$ and $\mathbf{V}$ are both square orthogonal matrices of dimensions $n \times n$ and $m \times m$, respectively, while Σ is a $n \times m$ diagonal matrix containing the singular values. Equation (9) will be satisfied if $\mathbf{z}_0 > \mathbf{0}$ or $\mathbf{z}_0 < \mathbf{0}$. This condition is used in this paper to compute the approximate WCW of planar parallel CDMs with four cables. The three-dimensional WCW is represented by a set of two-dimensional slices corresponding to different orientations ϕ. For a given orientation of the EE, the constant orientation wrench closure workspace (COWCW), when it exists, is a bounded area of the XY plane. An area of the XY plane known to encompass the COWCW is thus discretized into a point cloud. Each point is then verified against the conditions expressed in (8) and (9). The set of points satisfying the conditions represent the COWCW. Moreover, the approximate boundary of the COWCW can be plotted by drawing lines through those points which are located on the boundaries of the set of points found to be in the COWCW. The procedure is then repeated for different values of ϕ to obtain an approximation of the WCW. It is recognized that this approach is not as optimal as, for instance, the use of interval analysis techniques (*e.g.* [9]) but it is deemed adequate for the purpose of this paper.

IV. COMPUTATION OF THE PRESTRESS STABLE WRENCH CLOSURE WORKSPACE

A relationship between infinitesimal changes in the total wrench applied to the mechanism's EE by the environment and the corresponding displacement of the EE can be formulated as follows

$$\delta\mathbf{w}_e = \begin{bmatrix} \delta\mathbf{f} \\ \delta M \end{bmatrix} = \mathbf{K} \begin{bmatrix} \delta\mathbf{p} \\ \delta\phi \end{bmatrix} = \mathbf{K}\delta\mathbf{x} \tag{10}$$

where $\mathbf{K}$ is the mechanism's 3×3 stiffness matrix. Given a state of the mechanism where static equilibrium is achieved (*i.e.*, (5) and (6) are satisfied), stability of the mechanism implies that positive work must be done on the mechanism to displace it away from its equilibrium. This condition may be expressed as

$$\delta\mathbf{w}_e^T\delta\mathbf{x} = (\mathbf{K}\delta\mathbf{x})^T\delta\mathbf{x} = \delta\mathbf{x}^T\mathbf{K}\delta\mathbf{x} > 0, \tag{11}$$

which makes it clear that for stability to exist $\mathbf{K}$ must be positive definite.

The stiffness of general planar parallel CDMs with four cables is to be modeled here by considering the mechanism's flexibility to stem only from the compliance of its cables (in fact the stiffness model that will be derived is applicable to planar parallel CDMs with any number of cables). The latter are modelled as linear springs such that

$$t_i = k_i(l_i - l_{0_i}) \tag{12}$$

where k_i and l_{0_i} are the axial stiffness and rest length of the ith cable, respectively. Different methods may be employed to compute the stiffness matrix of a CDM including the application of a conservative congruence transformation (CCT) [10], the use of virtual springs [6], the computation of the Hessian of the potential energy function of the mechanism, etc. In what follows, $\mathbf{K}$ is obtained using an approach inspired from Svinin *et al.* [8] based on the linearization of the static equilibrium equations. This approach is general, simple to apply and yields a compact expression for $\mathbf{K}$. The linearization of (5) leads to

$$\delta\mathbf{f} = -\sum_{i=1}^{4}(\delta t_i\mathbf{n}_i + t_i\delta\mathbf{n}_i). \tag{13}$$

It can be noticed from (12) that $\delta t_i = k_i\delta l_i$. In addition, any change in $\mathbf{n}_i$ must be due only to its rotation such that $\delta\mathbf{n}_i = \delta\theta_i\mathbf{E}\mathbf{n}_i$ where θ_i is the angle measured from the X axis to the line defined by the ith cable as shown in Fig. 1. Substituting these results into (13) offers the following

$$\delta\mathbf{f} = -\sum_{i=1}^{4}(k_i\delta l_i\mathbf{n}_i + t_i\delta\theta_i\mathbf{E}\mathbf{n}_i). \tag{14}$$

Expressions are now required for δl_i and $\delta\theta_i$ in terms of $\delta\mathbf{p}$ and $\delta\phi$. Referring to Fig. 1, the kinematic constraint related to the ith cable is written as

$$\mathbf{p} + \mathbf{b}_i = \mathbf{a}_i - l_i\mathbf{n}_i. \tag{15}$$

Observing that $\delta\mathbf{b}_i = \delta\phi\mathbf{E}\mathbf{b}_i$, the linearization of this expression leads to

$$\delta\mathbf{p} + \delta\phi\mathbf{E}\mathbf{b}_i = -\delta l_i\mathbf{n}_i - l_i\delta\theta_i\mathbf{E}\mathbf{n}_i. \tag{16}$$

Multiplying both sides of this equation by $\mathbf{n}_i^T$ leads to

$$\delta l_i = -\mathbf{n}_i^T(\delta\mathbf{p} + \delta\phi\mathbf{E}\mathbf{b}_i). \tag{17}$$

Moreover, multiplying both sides of the same equation by $(\mathbf{E}\mathbf{n}_i)^T$ yields

$$\delta\theta_i = -\frac{1}{l_i}(\mathbf{n}_i^T\mathbf{E}^T\delta\mathbf{p} + \mathbf{n}_i^T\mathbf{b}_i\delta\phi). \tag{18}$$

Substituting the results of (17) and (18) into (14) and simplifying, an expression for $\delta\mathbf{f}$ in terms of a small displacement of the EE is finally obtained as

$$\begin{aligned}\delta\mathbf{f} = &\left[\sum_{i=1}^{4}k_i\mathbf{n}_i\mathbf{n}_i^T\right]\delta\mathbf{p} + \left[\sum_{i=1}^{4}k_i\mathbf{n}_i\mathbf{n}_i^T\mathbf{E}\mathbf{b}_i\right]\delta\phi \\ &+ \left[\sum_{i=1}^{4}\frac{t_i}{l_i}\mathbf{E}\mathbf{n}_i\mathbf{n}_i^T\mathbf{E}^T\right]\delta\mathbf{p} + \left[\sum_{i=1}^{4}\frac{t_i}{l_i}\mathbf{E}\mathbf{n}_i\mathbf{n}_i^T\mathbf{b}_i\right]\delta\phi\end{aligned} \tag{19}$$

Meanwhile, the linearization of (6) results in

$$\delta M = -\sum_{i=1}^{4}(\delta t_i\mathbf{b}_i^T\mathbf{E}^T\mathbf{n}_i + t_i\delta\mathbf{b}_i^T\mathbf{E}^T\mathbf{n}_i + t_i\mathbf{b}_i^T\mathbf{E}^T\delta\mathbf{n}_i). \tag{20}$$

Substituting previously stated expressions for δt_i, $\delta\mathbf{b}_i$ and $\delta\mathbf{n}_i$ as well as (17) and (18), the following result is obtained

$$\begin{aligned}\delta M = &\left[\sum_{i=1}^{4}k_i\mathbf{b}_i^T\mathbf{E}^T\mathbf{n}_i\mathbf{n}_i^T\right]\delta\mathbf{p} + \left[\sum_{i=1}^{4}k_i\mathbf{b}_i^T\mathbf{E}^T\mathbf{n}_i\mathbf{n}_i^T\mathbf{E}\mathbf{b}_i\right]\delta\phi \\ &+ \left[\sum_{i=1}^{4}\frac{t_i}{l_i}\mathbf{b}_i^T\mathbf{n}_i\mathbf{n}_i^T\mathbf{E}^T\right]\delta\mathbf{p} + \left[\sum_{i=1}^{4}\frac{t_i}{l_i}\mathbf{b}_i^T\mathbf{n}_i\mathbf{n}_i^T\mathbf{b}_i\right]\delta\phi \\ &+ \left[\sum_{i=1}^{4}t_i\mathbf{b}_i^T\mathbf{n}_i\right]\delta\phi\end{aligned} \tag{21}$$

Finally, referring to (10), an expression for the mechanism's stiffness matrix is obtained as $\mathbf{K} = \mathbf{K}_k + \mathbf{K_t}$ where

$$\mathbf{K}_k = \sum_{i=1}^{4} k_i \begin{bmatrix} \mathbf{n}_i\mathbf{n}_i^T & \mathbf{n}_i\mathbf{n}_i^T\mathbf{E}\mathbf{b}_i \\ \mathbf{b}_i^T\mathbf{E}^T\mathbf{n}_i\mathbf{n}_i^T & \mathbf{b}_i^T\mathbf{E}^T\mathbf{n}_i\mathbf{n}_i^T\mathbf{E}\mathbf{b}_i \end{bmatrix} \tag{22}$$

$$\mathbf{K_t} = \sum_{i=1}^{4} \frac{t_i}{l_i} \begin{bmatrix} \mathbf{E}\mathbf{n}_i\mathbf{n}_i^T\mathbf{E}^T & \mathbf{E}\mathbf{n}_i\mathbf{n}_i^T\mathbf{b}_i \\ \mathbf{b}_i^T\mathbf{n}_i\mathbf{n}_i^T\mathbf{E}^T & \mathbf{b}_i^T\mathbf{n}_i\mathbf{n}_i^T\mathbf{b}_i \end{bmatrix} + \sum_{i=1}^{4} t_i \begin{bmatrix} \mathbf{0}_{2\times 2} & \mathbf{0}_{2\times 1} \\ \mathbf{0}_{1\times 2} & \mathbf{b}_i^T\mathbf{n}_i \end{bmatrix} \tag{23}$$

and where $\mathbf{0}_{r\times s}$ is the $r \times s$ zero matrix. It is mentioned that this result has been validated with stiffness matrices computed using both the CCT [10] and the potential energy formulations.

The contribution of the individual axial stiffness of the mechanism's cables to its overall stiffness is represented by matrix $\mathbf{K}_K$. In fact, (22) can be shown to correspond to $\mathbf{K}_k = \mathbf{J}^T\mathbf{K}_c\mathbf{J}$ where $\mathbf{J} = -\mathbf{W}^T$ is the mechanism's Jacobian matrix and $\mathbf{K}_c = \text{diag}([k_1, k_2, \ldots, k_m])$ is a diagonal matrix containing the cables' axial stiffness coefficients. As long as the individual cable stiffness coefficients are positive and the mechanism is in its WCW, $\mathbf{K}_k$ is seen to be positive definite. Meanwhile, matrix $\mathbf{K_t}$ corresponds to the portion of the mechanism's overall stiffness that is generated by its prestress. It is seen to be linearly proportional to the cable tensions and can be rewritten as $\mathbf{K_t} = \mathbf{K_{t_w}} + \mathbf{K_{t_0}}$ where $\mathbf{K_{t_w}}$ is the portion of $\mathbf{K_t}$ due to $\mathbf{t_w}$ while $\mathbf{K_{t_0}}$ depends on $\mathbf{t}_0$. It is useful here to recall from section III that $\mathbf{t_w}$ is the vector of cable tensions required to equilibrate the wrench applied to the EE while $\mathbf{t}_0$ is the vector of cable tensions due to the mechanism's prestress. Both $\mathbf{K_{t_w}}$ and $\mathbf{K_{t_0}}$ can be negative definite depending on the mechanism's geometry and configuration as well as the external wrench applied to the EE. With this in mind, the PSWCW is defined as the subset of the WCW where, in each configuration, the mechanism's stiffness matrix can be made positive definite (and thus the mechanism stabilized) under any arbitrary (but finite in magnitude) external load simply by increasing the level of prestress (by increasing λ in (7)). Such configurations were termed "stabilizable" in [6]. This condition can only be satisfied if $\mathbf{K_{t_0}}$ is itself positive definite, *i.e.*, the stiffness must increase when the level of prestress is increased. Based on the fact that one has complete control over the prestress level, the overall stiffness matrix $\mathbf{K}$ can thus be made positive definite regardless of the positive definiteness of $\mathbf{K_{t_w}}$ by ensuring that the prestress tension forces are high enough.

In this work, the PSWCW is approximated using an approach equivalent to the one described in section III for the WCW (*i.e.*, by combining slices of constant orientation). A configuration is deemed to be in the PSWCW if $\mathbf{K_{t_0}}$, evaluated at the configuration, is positive definite. This is determined by computing the eigenvalues of $\mathbf{K_{t_0}}$ and verifying that they are all strictly positive. While the specific value of $\mathbf{t}_0$ that is used to compute $\mathbf{K_{t_0}}$ is not important, it is important that $\mathbf{t}_0$ be in the nullspace of $\mathbf{W}$. For this reason, $\mathbf{t}_0 = |\mathbf{z}_0|$ is used where $|\mathbf{z}_0|$ is to be interpreted as $\mathbf{z}_0$ if $\mathbf{z}_0 > \mathbf{0}$ and $-\mathbf{z}_0$ otherwise (it is already known from the WCW condition that $\mathbf{z}_0 > \mathbf{0}$ or $\mathbf{z}_0 < \mathbf{0}$).

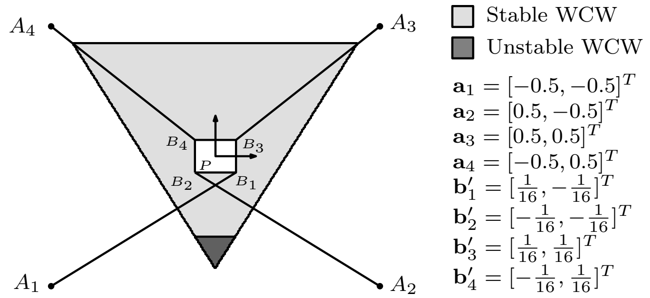

Fig. 2. Example of a planar parallel CDM with unstable configurations within its WCW (prestrain of 2.5%).

V. RESULTS

Since $\mathbf{K}_k$ is positive definite, a planar parallel CDM does not become unstable simply because $\mathbf{K_{t_w}}$ and $\mathbf{K_{t_0}}$ may be negative definite. In fact, $\mathbf{K}_k$ very often dominates numerically over $\mathbf{K_{t_w}}$ and $\mathbf{K_{t_0}}$ such that it is worthwhile to question whether $\mathbf{K}$ may ever become negative definite under normal circumstances. This question is addressed by way of an example of a mechanism, shown in Fig. 2 along with a sketch of its WCW, that becomes unstable due to the application of prestress in its cables. For the computation of this result, the cable stiffness was set to $k_i = 1/l_{0_i}$ which, looking at (12), leads one to observe that $\tau_i = \varepsilon_i$ where $\varepsilon_i = (l_i - l_{0_i})/l_{0_i}$ is the strain in the ith cable. The cable forces were due to prestress only (*i.e.*, no external wrench was applied) and the maximum tension was set to 0.025 which corresponds to a 2.5% strain. Under these conditions, the mechanism becomes unstable in a triangular region at the bottom of its WCW (despite the fact that $\mathbf{K}_k$ remains positive definite).

Prior to presenting optimization results, it is also interesting to look at an example of a mechanism where the difference between the WCW and the PSWCW is significant. One such mechanism whose base and EE cable attachment points are both positioned on the vertex of squares is represented in Fig. 3. From the perspective of the WCW, this mechanism is very attractive. However, only approximately 23% of the WCW also belongs to the PSWCW. The results provided in Figs. 2 and 3 make it clear that if the ability to increase the stiffness of a planar parallel CDM by modifying the level of prestress in order to avoid instabilities is deemed desirable, then designing mechanisms with the PSWCW in mind is necessary.

A genetic algorithm (GA) [11] was used to optimize the planar parallel CDM's geometry with the objective of having a desired PSWCW for a fixed orientation $\phi = 0$. A GA is an intelligent random search algorithm that is based on the principles of evolution and natural selection inspired by Charles Darwin's survival of the fittest theory. Compared with gradient-based search algorithms, the GA does not require the derivative of the function being optimized and it is less susceptible to converge to local optima. Moreover, it has been used successfully in the past to perform the optimization of parallel CDMs [9, 12]. The desired workspace was chosen

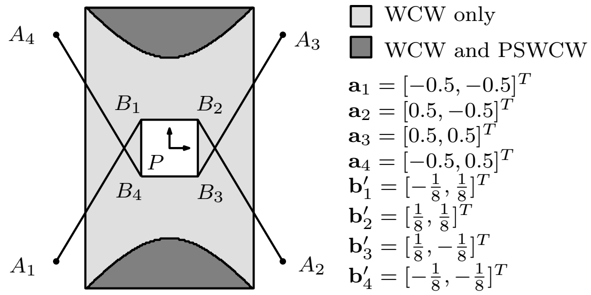

Fig. 3. Comparison of the WCW and PSWCW for a typical planar parallel CDM with four cables.

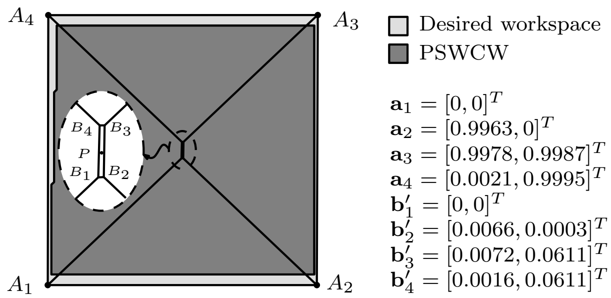

Fig. 4. General planar parallel CDM optimized with the GA for $\phi = 0$.

as a square defined by $0 \leq x \leq 1$ and $0 \leq y \leq 1$. In order to minimize the dimension of the search space without sacrificing the generality of mechanism's geometry, node A_1 was assumed to be coincident with the origin of the XY frame while A_2 was constrained to the X axis. Node B_1 was also assumed to be coincident with the origin of frame $X'Y'$. However, the position of point P used to compute the PSWCW was chosen at the geometrical centre of the B_i nodes. A total of 11 parameters were thus used to represent the system, *i.e.*, $\mathbf{x} = [a_{2_x}, a_{3_x}, a_{3_y}, a_{4_x}, a_{4_y}, b_{2_x}, b_{2_y}, b_{3_x}, b_{3_y}, b_{4_x}, b_{4_y}]^T$. The bounded range for all A_i nodal coordinates was $[0,1]$ while that for the B_i nodes was $[-0.5, 0.5]$. The fitness function used was $\eta = -N/N_g$ where $N_g = 900$ is the number of points in the grid that was used to represent the desired workspace and N is the number of points from that grid which satisfy the PSWCW conditions. One can observe that $0 \leq |\eta| \leq 1$ represents the fraction of the desired workspace that belongs to the PSWCW. A representative result generated by the GA is shown in Fig. 4. In this case, the PSWCW covers approximately 87% of the desired workspace and it can be seen that the EE's geometry is approaching that of a line. In fact, this is not quite the optimal geometry. Theoretically, the fraction of the PSWCW that covers the desired workspace will go to 100% as the EE geometry degenerates *toward* a point. The GA did not find this result due to the dimension of the search space as well as the numerical nature of the PSWCW computation.

Although optimal, the mechanism generated by the GA shown in Fig. 4 is not practical for most applications due to the geometry of its EE. Moreover, since the synthesis is being performed with no particular application in mind, symmetry is a desirable property which can be imposed. An

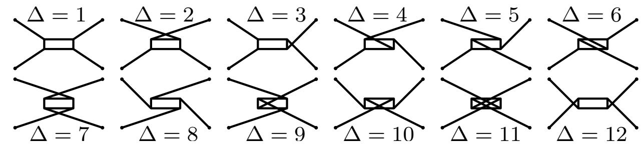

Fig. 5. Possible cable connectivities.

analysis of the PSWCW was thus performed for symmetric mechanism geometries where the EE is constrained to a rectangular shape and the cable attachment points on the base are positioned at coordinates (0,0), (1,0), (1,1) and (0,1) (*i.e.*, the corner's of the desired workspace). The mechanism's geometry in this case is represented by the width (w) and the height to width ratio (α) of its EE in addition to an index Δ used to represent the connectivity of the cables to the EE. There are 24 ways by which the four cables can be connected to the EE. Of these, only 12 are unique in terms of their PSWCW due to symmetry considerations. These are illustrated in Fig. 5. In Fig. 6, the fraction of the desired workspace that belongs to the PSWCW is plotted for different cable connectivities with $\alpha \in [0,1]$ and $w = [0.1, 0.4, 0.7]$. To maintain the clarity of the plots, only the connectivities represented by $\Delta = 1$, 2, 3 and 12 are shown as they are the most promising. The plots indicate that the size of the PSWCW is inversely proportional to w, a result which is in concordance with the geometry previously found by the GA in Fig. 4. Moreover, it is observed that the connectivities that are most promising with respect to the PSWCW are those represented by $\Delta = 1$, 2, 3 and 12. Of these, the case with no cables crossing ($\Delta = 1$) is consistently the one with the largest PSWCW. However, when $\alpha = 1$, the PSWCW of mechanisms with $\Delta = 1$ connectivity (as well as the WCW for that matter) does not exist. Moreover, it is reiterated that these results consider a constant orientation $\phi = 0$ and that mechanisms with no cables crossing (*e.g.* $\Delta = 1$) tend to have very limited reachable EE orientation ranges.

The GA was also used to investigate the optimal mechanism geometry when the EE is to operate in a range of orientations. For this purpose, the symmetry of the mechanism was once again imposed with its geometry being represented by $w \in [0.1, 0.5]$, $\alpha \in [0.25, 1]$ and $\Delta = 1, 2, \ldots, 12$ where the allowable parameter ranges or values are indicated. The desired workspace was set to a parallelepiped defined by $0 \leq x \leq 1$, $0 \leq y \leq 1$ and $-\pi/6 \leq \phi \leq \pi/6$. For a given orientation ϕ_j, a grid containing $N_g = 2500$ points is created to span the area of the desired constant orientation workspace in the XY plane. The number of points from the grid that satisfy the PSWCW conditions, N_{ϕ_j}, is then computed. Based on this, the fitness function is set to $\eta = -\min(\eta_j)$ with $\eta_j = N_{\phi_j}/N_g$ and where orientations $\phi = -\pi/6$, $-\pi/12$, 0, $\pi/12$ and $\pi/6$ radians were considered. In other words, the GA seeks to optimize the mechanism's geometry such that the fraction of the desired constant orientation workspace belonging to the constant orientation PSWCW of the mechanism for the orientation having the poorest performance is

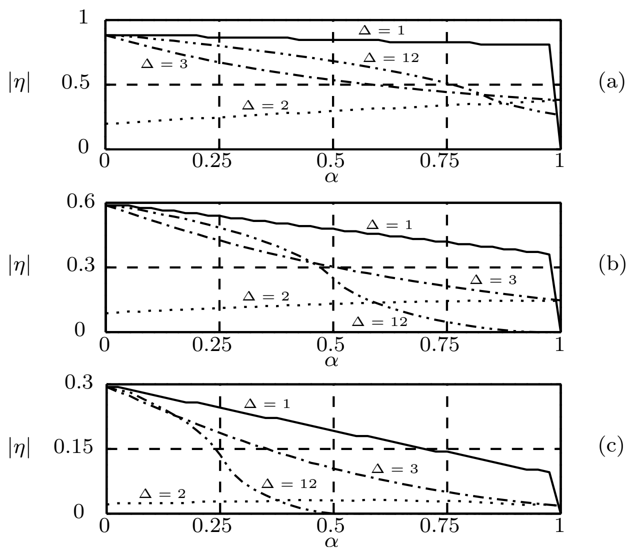

Fig. 6. Plot of the fraction of the desired workspace contained in the PSWCW as a function of α: a) $w = 0.1$, b) $w = 0.4$ and c) $w = 0.7$.

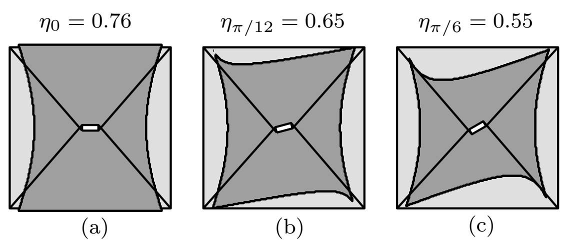

Fig. 7. PSWCW of an optimized symmetric mechanism with $w = 0.1011$, $\alpha = 0.3413$ and $\Delta = 12$ a) $\phi = 0$, b) $\phi = \pi/12$ and c) $\phi = \pi/6$ radians.

maximized. The optimized mechanism is shown along with its constant orientation PSWCW for different orientations in Fig. 7 (results for $\phi < 0$ are qualitatively equivalent to those for $\phi > 0$ due to the mechanism's symmetry). As expected, the $\Delta = 1$ connectivity, although the best when $\phi = 0$ is considered, is not optimal when the mechanism is to operate in a range of orientations.

VI. CONCLUSION

It is known that parallel CDMs may become unstable in some configurations of their WCW due to the internal forces in their cables that are generated by prestress or by external loads applied to the EE. With this in mind, the PSWCW is defined as the subset of the WCW for which the mechanism stiffness may be increased by increasing the level of prestress. The stability of the mechanism can be guaranteed in such configurations regardless of the external load by maintaining a sufficient prestress level. In this paper, the synthesis of planar parallel CDMs with four cables is performed using a GA with the objective of obtaining a prescribed PSWCW. From the results that are obtained, a few general guidelines can be extracted and used in a preliminary design context. For instance, not unexpectedly, mechanisms whose EE is small with respect to the polygon formed by the attachment points of the cables to the base tend to have a larger PSWCW. Meanwhile, mechanisms with no cables crossing prove to be best when only a fixed orientation is considered while mechanisms with double cable crossing are better when mechanisms must operate in a range of orientations (note that the latter result is contingent on the size of the EE and may change if the latter is increased). The generalization of the synthesis approach for cases where $m > 4$ as well as the inclusion of other mechanism performance criteria (*e.g.* stiffness) is left to future work.

REFERENCES

[1] A. Ming and T. Higuchi, "Study on multiple degree-of-freedom position mechanism using wires (part 1)," *International Journal of the Japanese Society for Precision Engineering*, vol. 28, no. 2, pp. 131–138, 1994.

[2] G. Barrette and C. M. Gosselin, "Determination of the dynamic workspace of cable-driven planar parallel mechanisms," *Journal of Mechanical Design, Transactions of the ASME*, vol. 127, no. 2, pp. 242–248, 2005.

[3] P. Bosscher and I. Ebert-Uphoff, "Wrench-based analysis of cable-driven robots," in *Proceedings - IEEE International Conference on Robotics and Automation*, New Orleans, LA, United States, 2004, pp. 4950–4955.

[4] M. Gouttefarde and C. M. Gosselin, "Analysis of the wrench-closure workspace of planar parallel cable-driven mechanisms," *IEEE Transactions on Robotics*, vol. 22, no. 3, pp. 434–445, 2006.

[5] C. Sui and M. Zhao, "Study on a 3-DOF parallel wire driven lightweight flexible manipulator: kinematics, statics and stiffness," in *Proceedings of the 2004 International Conference on Manipulation and Grasping (IMG'04)*, 2004.

[6] S. Behzadipour and A. Khajepour, "Stiffness of cable-based parallel manipulators with application to stability analysis," *Journal of Mechanical Design, Transactions of the ASME*, vol. 128, no. 1, pp. 303–310, 2006.

[7] S. Sahin and L. Notash, "Force and stiffness analyses of wire-actuated parallel manipulators," in *Proceedings of the 12th IFToMM World Congress*, 2007.

[8] M. Svinin, S. Hosoe, and M. Uchiyama, "On the stiffness and stability of Gough-Stewart platforms," in *Proceedings - IEEE International Conference on Robotics and Automation*, Seoul, Republic of Korea, 2001, pp. 3268–3273.

[9] T. Bruckmann, L. Mikelsons, T. Brandt, M. Hiller, and D. Schramm, "Design approaches for wire robots," in *Proceedings of the ASME 2009 International Design Engineering Technical Conferences & Computers and Information in Engineering Conference*, 2009.

[10] C. Huang, W.-H. Hung, and I. Kao, "New conservative stiffness mapping for the Stewart-Gough platform," in *Proceedings - IEEE International Conference on Robotics and Automation*, Washington, DC, United States, 2002, pp. 823–828.

[11] D. E. Goldberg, *Genetic Algorithms in Search, Optimization, and Machine Learning*, 1st ed. Addison-Wesley Professional, 1989.

[12] C. Leclerc and C. M. Gosselin, "Algorithme génétique multicritériel pour l'optimisation de l'architecture des mécanismes entraînés par câbles – application à un simulateur de vol," in *Proceedings of the CCToMM Symposium on Mechanisms, Machines and Mechatronics*, 2009.